RESEARCH ARTICLE

Key Points:
- Sea level rise increases the salinity of the Baltic Sea
- This increase is related to more frequent and stronger salt inflows
- One notices a decreased mixing and a bigger cross section in the Danish Straits

Influence of sea level rise on the dynamics of salt inflows in the Baltic Sea

Robinson Hordoir[1], Lars Axell[1], Ulrike Löptien[2], Heiner Dietze[2], and Ivan Kuznetsov[3]

[1]Department of Oceanography Research, SMHI, Norrköping, Sweden, [2]GEOMAR Helmholtz-Zentrum für Ozeanforschung, Kiel, Germany, [3]Institute of Coastal Research, Helmholtz-Zentrum Geesthacht, Geesthacht, Germany

Abstract The Baltic Sea is a marginal sea, located in a highly industrialized region in Central Northern Europe. Saltwater inflows from the North Sea and associated ventilation of the deep exert crucial control on the entire Baltic Sea ecosystem. This study explores the impact of anticipated sea level changes on the dynamics of those inflows. We use a numerical oceanic general circulation model covering both the Baltic and the North Sea. The model successfully retraces the essential ventilation dynamics throughout the period 1961–2007. A suite of idealized experiments suggests that rising sea level is associated with intensified ventilation as saltwater inflows become stronger, longer, and more frequent. Expressed quantitatively as a salinity increase in the deep central Baltic Sea, we find that a sea level rise of 1 m triggers a saltening of more than 1 PSU. This substantial increase in ventilation is the consequence of the increasing cross section in the Danish Straits amplified by a reduction of vertical mixing.

1. Introduction

The Baltic Sea is a semienclosed basin. River inflows from highly industrialized countries determine its brackish characteristic and render it vulnerable to anthropogenic eutrophication. It is a highly stratified estuary and its lower layers can only receive oxygen by salinity intrusions finding their way through three narrow passages linking the Baltic with the North Sea, the so-called Danish Straits. These three straits are called, from West toward East "Little Belt," "Great Belt," and "Öresund," and have different vertical cross sections (Figure 1). The middle strait (Great Belt) is the broadest and deepest, hosting the largest share of the exchange.

The inflowing water is typically characterized by a relatively high salinity and a high oxygen content. Thus, saltwater inflows from the North Sea are a vital source of oxygen for the Baltic Sea and the whole ecosystem is impacted by their frequency and intensity.

Salt inflows directly influence the salinity structure of the Baltic Sea [*Meier*, 2007; *Meier and Kauker*, 2003; *Meier et al.*, 2003; *Lass and Matthäus*, 1996]. They also influence biological processes such as cod spawning [*Stigebrandt et al.*, 2014] and the ventilation of the deeper layers of the Baltic Sea is crucial to macrobenthic organisms [*Gogina and Zettler*, 2010]. Previous studies have shown that the frequency of saltwater inflows has decreased during the recent decades, particularly in the period between 1983 and 1993 [*Lass and Matthäus*, 1996]. Saltwater inflows are also suspected to decrease in a future climate due to an increase of the runoff into the Baltic Sea [*Meier et al.*, 2006]. Hypoxia is nowadays a severe environmental problem for the Baltic Sea, reaching a point where even geoengineering solutions are under discussion [*Stigebrandt et al.*, 2014]. Additionally, the high nutrient content of the Baltic Sea together with increased temperatures suggest that the lower layers are prone to reach a state of hypoxia more often and with a greater extent [*Meier et al.*, 2012].

The impact of sea level rise on the Baltic Sea haline dynamics has, so far, not been investigated, and one challenging question is to determine how the Baltic Sea salt inflow dynamics respond to a significant sea level increase: the aim of this article is to address this issue. Based on a coupled ocean-sea ice model configuration with a fully nonlinear free surface, covering the Baltic Sea and the North Sea, we perform a suite of sensitivity experiments. We compare the dynamics of Baltic Sea salt inflows between a present-day sea level and several levels of sea level increase.
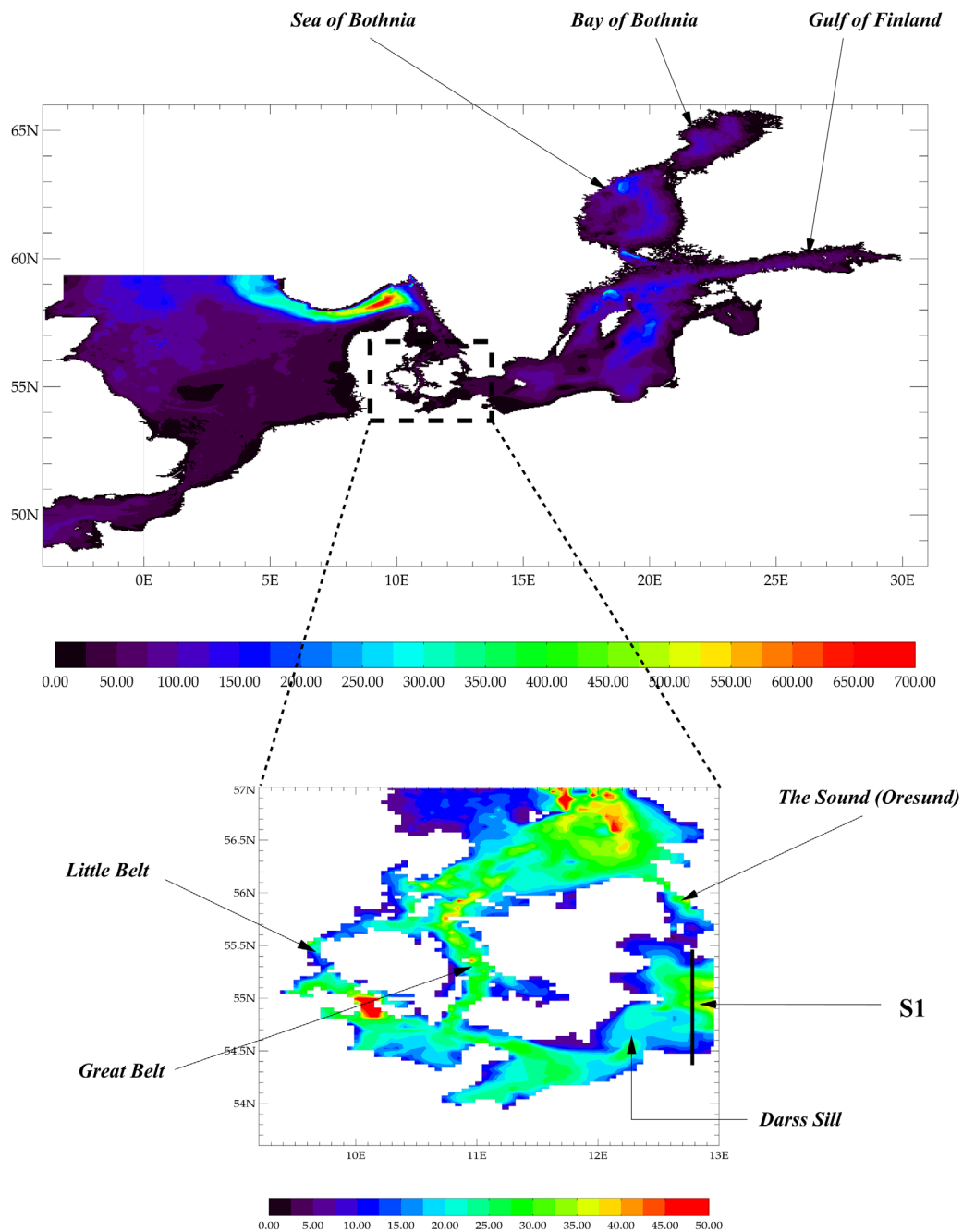
Figure 1. Geographical domain and color map of bathymetry (in m) of the NEMO-Nordic configuration, with zoom on the Danish Straits area between Denmark and Sweden, and position of the S1 cross section.

The second section of this article introduces the model setup and includes an evaluation of the haline dynamics. In the third section, we present the results of the sensitivity experiments. In the fourth section, we present a theoretical approach which tackles the problem from a process-orientated perspective. The fifth and final section comprises a final discussion and our conclusions.

2. Methodology

2.1. NEMO-Nordic: A NEMO-Based Ocean Modeling Configuration for Baltic and North Seas

Our analyses are based on the NEMO-Nordic configuration developed at SMHI (Swedish Meteorological and Hydrological Institute) which has been used in previous studies (under the name BaltiX) [*Hordoir et al.*, 2013;

Godhe et al., 2013]. NEMO-Nordic is a coupled ocean-sea ice model based on the NEMO ocean engine [*Madec*, 2010]. Its domain includes the entire Baltic Sea basin, and a major part of the North Sea (Figure 1, the critical area of the Danish Straits is also shown in detail). NEMO-Nordic provides sea level predictions in operational mode reaching a higher level of quality than that of the HIROMB system [*Funkquist and Kleine*, 2007; *Axell et al.*, 2014] used for operational predictions at SMHI, a system that NEMO-Nordic is intended to replace. The domain of NEMO-Nordic is similar to that of HIROMB. With 56 vertical levels, it has a resolution of approximately 2 nautical miles (≈3700 m), and a vertical resolution of 3 m close to the surface, decreasing to 22 m at the bottom of the deepest part of the domain (Norwegian trench). NEMO-Nordic has two open boundaries: a meridional one located in the English Channel between Brittany and Cornwall, and a zonal one between Scotland and Norway [*Hordoir et al.*, 2013]. Since we use a resolution of 2 nautical miles, it is sometimes difficult to give each critical section of the Danish Straits its true width. Therefore, we have instead made each critical cross sections of each strait fit its actual measured size. To reach this goal, we have slightly modified either the depth or the width of each critical cross section, so that the surface of each critical cross section fits its actual size. This has been done with the goal to find the best compromise that modifies as little as possible depth or width.

NEMO-Nordic uses a fully nonlinear explicit free surface, based on the approach described by *Adcroft and Campin* [2004]. Partial steps are used in order to obtain a good consistency between the input bathymetry and that utilized by the model. We use a time-splitting approach that computes a barotropic and a baroclinic mode, as well as the interaction between them.

The barotropic mode is defined at the open boundary conditions using the Oregon State University Tidal Inversion Model [*Egbert et al.*, 1994; *Egbert and Erofeeva*, 2002] with 11 tidal harmonics defined both for sea level and barotropic tidal velocities. In addition, a simple coarse resolution barotropic storm surge model covering a large area of the Northern Atlantic basin provides wind-driven sea level that is added to the tidal contribution. The Levitus climatology [*Levitus and Boyer*, 1994] provides temperature and salinity data at the open boundary conditions. Simple radiation conditions are applied to calculate baroclinic velocities at these boundaries.

The surface boundary condition uses a bulk formulation based on *Large and Yeager* [2004]. The ocean model is coupled to the LIM3 sea ice model [*Vancoppenolle et al.*, 2008]. The sea-ice salinity is set to a constant value of 10^{-3} PSU. A quadratic friction is applied at the bottom, and the drag coefficient is computed for each bottom grid cell based on a classical law-of-the-wall, with a constant bottom roughness of 3 cm.

NEMO-Nordic uses a TVD advection scheme with a modified leapfrog approach that ensures a very high degree of tracer conservation [*Leclair and Madec*, 2009]. It uses a $k-\epsilon$ turbulence scheme to parameterize unresolved vertical turbulence [*Umlauf and Burchard*, 2003]. In addition, in order to obtain a stable long-term stratification for the Baltic Sea, the Galperin parameterization is used [*Galperin et al.*, 1988].

We apply a Laplacian isopycnal diffusion both for momentum and tracers with a diffusion parameter that is constant in time, but varies in space. Isopycnal viscosity is set to 50 m^2 s^{-1} between the sea surface and a depth of 30 m, and to 0.001 m^2 s^{-1} below 30 m. An additional strong isopycnal diffusion is used close to the Neva river inflow (Gulf of St. Petersburg) in order to avoid negative salinities. Our model does not necessitate any algorithm to artificially cut off spurious negative salinities.

We set the isopycnal diffusivity to 10% of the value of isopycnal viscosity, which proves to be a good compromise to insure a low viscosity and diffusivity while keeping the model barotropically and baroclinically stable.

However, this approach does not work well close to the bottom where higher diffusivity and viscosity would hamper salt inflows to the deepest layers of the Baltic Sea. Note that this is consistent with results from *Dietze et al.* [2014, Figure 15, bottom] who describe the antagonistic effects of viscosity. To obtain realistic results, we have set very low values for isopycnal diffusion and isopycnal viscosity below the mixed-layer depth. We also use a parameterization of the bottom boundary layer [*Beckmann and Döscher*, 1997] to ease the propagation of saltwater inflows between the Danish Straits and the deepest layers of the Baltic Sea. Sensitivity experiments showed that using a purely diffusive bottom boundary layer produces the best results to bring saltwater masses to the deepest parts of the Baltic Sea. Using a combination of advective and diffusive methods within the bottom boundary layer parameterization, or purely advective, produces

too much entrainment which defeats the purpose of the parameterization. Lateral boundaries do not create any friction as a free-slip option is used.

The model is driven by atmospheric forcing derived from a downscaled run of an ERA40 reanalysis for the period 1961–2007. The downscaling is based on the regional atmospheric model RCA3 [*Samuelsson et al.*, 2011] which uses the reanalysis data as boundary conditions. This atmospheric model output was used successfully as atmospheric forcing for a number of Baltic Sea models [*Dietze et al.*, 2014; *Löptien and Meier*, 2011; *Löptien et al.*, 2013].

A runoff database provides the river flow to NEMO-Nordic; it includes inter-annual variability for the Baltic Sea basin and is based on climatological values for the North Sea basin. The salinity of the river runoff is set to a constant value of 10^{-3} PSU, which is the same value used for the sea-ice to avoid any negative salinity.

2.1.1. Evaluation of the Haline Dynamics of the Baltic Sea

Figure 2 shows climatological sea surface salinity (SSS hereafter) simulated from 1961 to 2007 by NEMO-Nordic, as well as the observed climatological SSS. The SSS is shown for March and July, which are the saltiest and freshest months of the year, respectively [*Eilola and Stigebrandt*, 1998; *Hordoir and Meier*, 2010]. The positions of the iso-salinity lines are in good agreement between the model and the observations, indicating that the model is capable of reproducing the seasonal cycle and the long-term averages in SSS. The iso-halines follow the freshwater seasonal cycle, with a deeper penetration of salinity in March in the central Baltic Sea basin (Baltic proper), and a low penetration in July. These salinity changes are consistent with the strong wind-driven release of freshwater during spring, reported in earlier studies [*Hordoir and Meier*, 2010].

Using the SHARK database (Svensk Havsarkiv, SMHI, and other Swedish Institutes), we compare the haline structures of the simulation with measurements (Figure 3) at three measurement stations BY2 (Arkona), BY5 (Bornholm), and BY15 (Gotland Deep); their positions are indicated in Figure 2.

All of our simulations start with a spurious inflows. This is probably a consequence of the spatially homogeneous (and rather unrealistic) initial conditions of sea surface height. Right after the inflow, a spurious stagnation period with monotonically decreasing salinities succeeds. It is only after 1965 that the intrinsic model dynamics overcome the deficiencies in our (rather unconstrained) initial conditions and that the deep salinity of NEMO-Nordic starts to approach realistic conditions.

NEMO-Nordic reproduces the vertical structure of the Baltic Sea with some bias. Such biases are typical for z-level models. Dense water inflows penetrating the Baltic Sea follow the bottom and are well reproduced at the Arkona (BY2) measurement station.

After the first shelf break between the Arkona (BY2) and Bornholm (BY5) measurement stations, the dense water flow has problems to follow the bottom and drives excessive ventilation of the intermediate layers further up in the water column.

In order to compensate for this behavior, ocean models that include only the Baltic Sea like that of *Meier* [2007] have modified the bathymetry of the first subbasins in addition to using bottom boundary layer parameterizations [*Beckmann and Döscher*, 1997] as in the present model.

The slight overventilation of the intermediate layers is responsible for two features that appear at the BY15 measurement station (Gotland Deep), located in the deepest place of the Baltic Sea along the inflow pathway. First, the overall salinity structure at BY15 is well reproduced, but the depth of the halocline is too shallow, located between 40 m and 50 m, whereas it should be at 60 m according to measurements. This also suggests a slight overventilation at the level of the halocline or even above it. Second, the bottom salinity is underestimated, with a negative bias peaking at 1.5 PSU in 2007. The fact that the bias is highest at the end of the simulation is specifically related with the underestimated major saltwater inflow in 2003. It is not related with the length of the simulation. The bias at the end of stagnation period for example, or after the 1993 major salt inflow, is lower.

This means that the model is able to preserve the haline structure of the Baltic Sea over a long time period. The ability of the model to reproduce major saltwater inflows is a key feature indispensable to maintaining realistic salinity in the deeper layers. This ability varies as the 1993 major inflow is, for example, well reproduced in terms of amplitude, whereas the 2003 major inflow is not. In the latter case, previous experience with the RCO model [*Meier et al.*, 2003; *Meier and Kauker*, 2003] suggests this specific inflow is difficult to
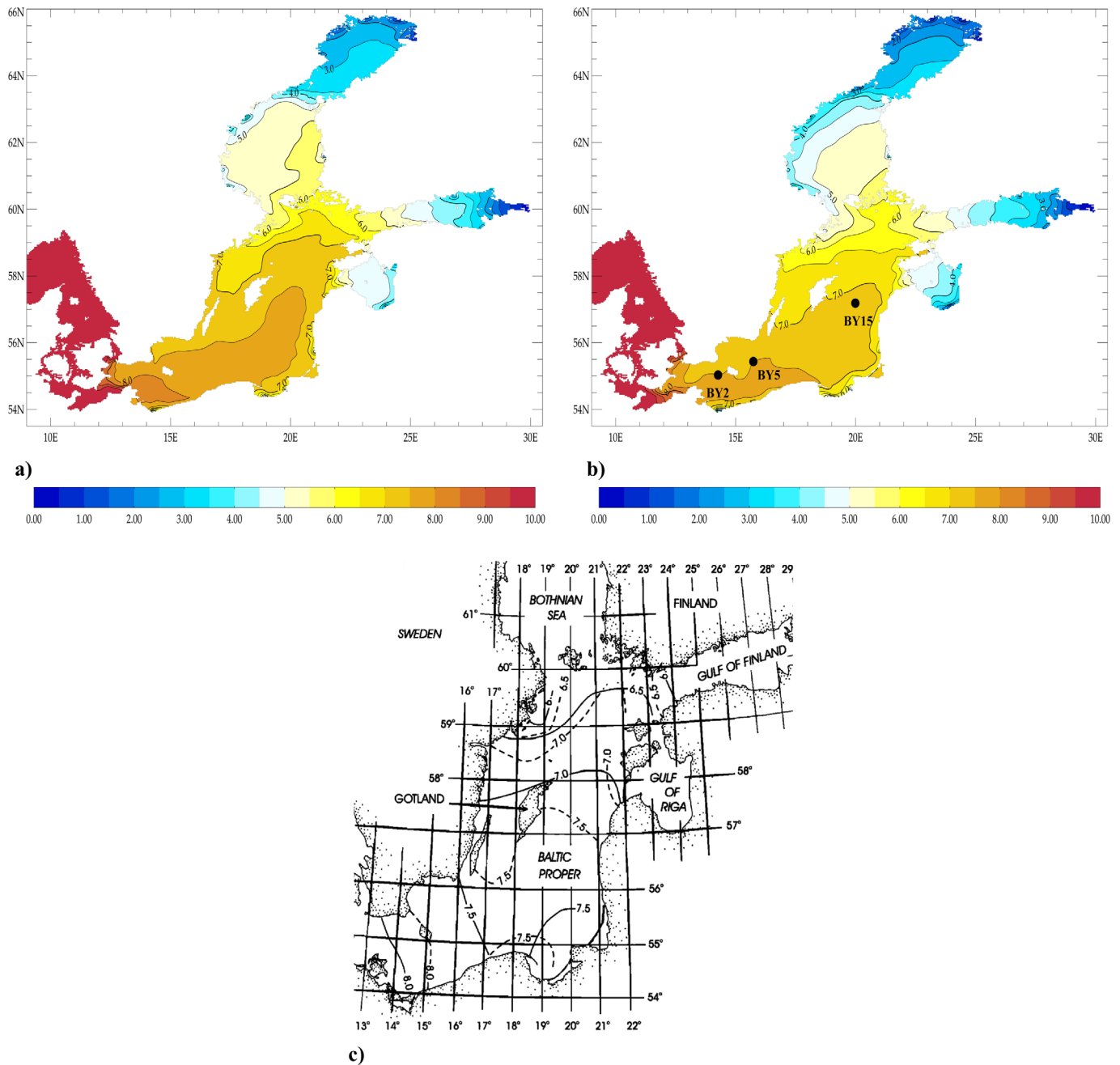
Figure 2. NEMO-Nordic simulated climatological sea surface salinities (in PSU) for the Baltic Sea for the months of (a) March and (b) July. (c) Observed climatological sea surface salinities [from *Eilola and Stigebrandt*, 1998]. Dashed lines, July; solid lines, March.

represent and cannot even be predicted based on the usual patterns in atmospheric circulation in contrast to other inflows [*Schimanke et al.*, 2014].

2.2. Sensitivity Experiments

Based on the NEMO-Nordic configuration run presented in section 2.1, we design a set of six experiments called e0, e0.5, e0.75, e1, e1.25, and e1.5. e0 is the reference experiment which corresponds to the standard long-term NEMO-Nordic simulation presented in section 2.1. The experiments e0.5, e0.75, e1, e1.25, and e1.5 differ from e0 only with respect to sea level. In each experiment, the mean sea level is increased by 0.5, 0.75, 1, 1.25, and 1.5 m for the experiments e0.5, e0.75, e1, e1.25, and e1.5, respectively. These values are
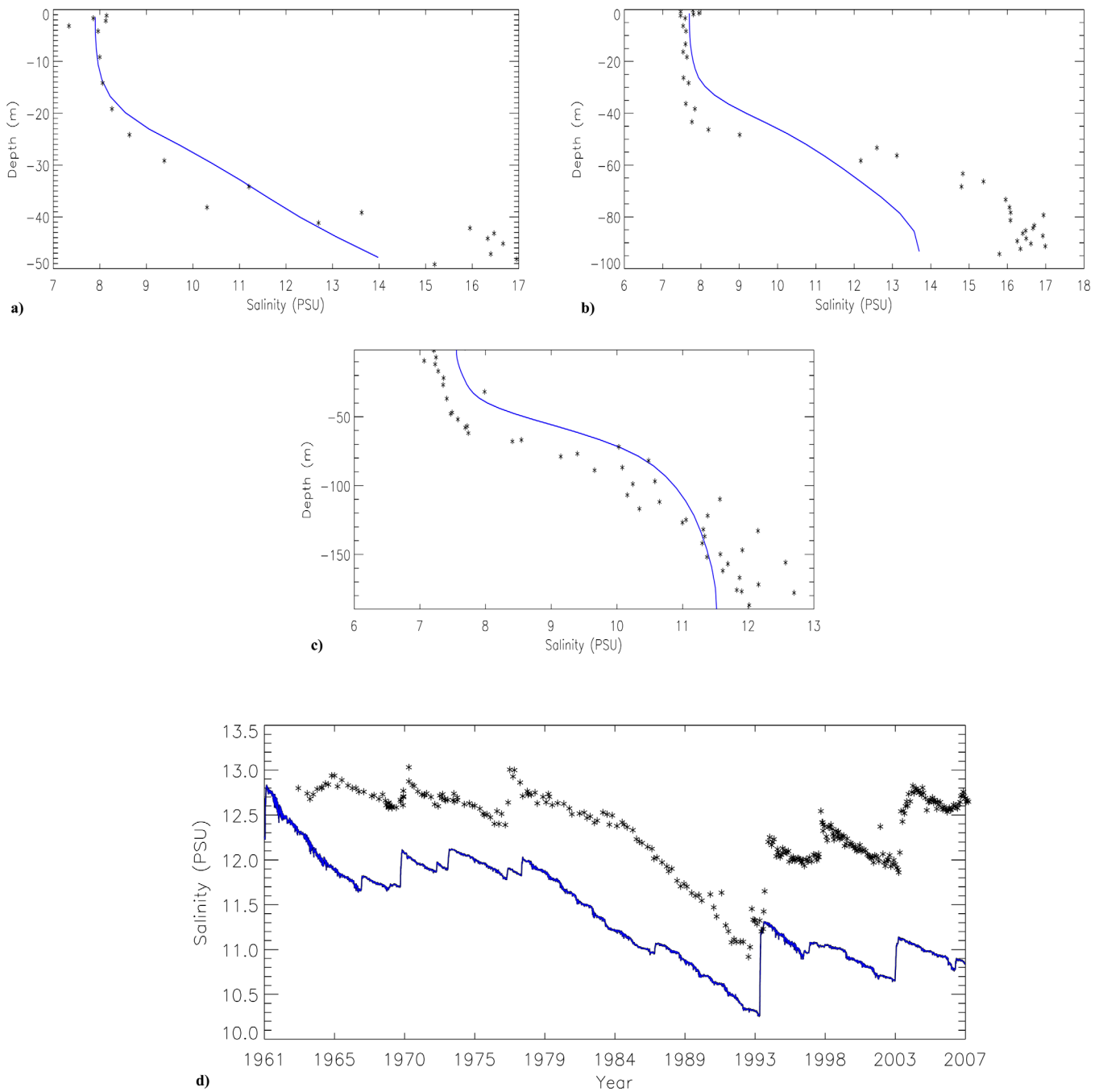
Figure 3. Salinity profiles (PSU) for the period 1961–2007 at stations (a) BY2, (b) BY5, and (c) BY15. (d) Deep salinity (PSU) at BY15 for the period 1961–2007.

taken based on the estimates made by *Blank et al*. [2012]. Their estimates suggest that there is a 95% chance that mean global sea level will increase by between 20 cm and 2 m by the end of the 21st century.

Although it remains to be shown how authorative such forecasts are in general, this seems to be consistent with other studies, e.g., *Pfeffer et al*. [2008] project a sea level rise of 78 cm–2 m based on the kinematics of glacial melt and *IPCC* [2013] project a global sea level increase between 25 cm and 1 m. How these global averages will be modulated by local wind patterns in the Baltic and North Sea is, however, not well constrained yet.

In addition to winds, land uplift may also contribute locally to the rise of sea levels in Baltic and North Sea [*Ekman and Mäkinen*, 1996]. However, this increase does not affect significantly the region of the Danish Straits which is key to inflow dynamics.

For pragmatic reasons we explore in this study the effects of a sea level rises that are of similar magnitude than anticipated global averages. Specifically, we assume that an increase of 0.5 m would be close to a lower-case scenario, whereas a value of 1.5 m would be close to an upper-case scenario. The elevated sea levels are prescribed in the model by changing the initial and boundary conditions. As for the latter, we add a respective bias to the storm surge model. The sea level rise value is also added to the initial conditions.

2.3. Diagnostics

In order to quantify volume and salt exchanges, we estimate the mean daily fluxes at a cross section. It is a meridional cross section located at the entrance of the Baltic Sea, east of Darss Sill (Figure 1) named S1. It captures the entire exchange between the North Sea and the Baltic Sea.

For any cross section C_s, we define the following diagnostics:

$$F_v(t) = \int_{C_s} \mathbf{u}(\mathbf{x}, t) \cdot \mathbf{dC_s}, \tag{1}$$

where $F_v(t)$ is the volume flux through the cross section C_s. $\mathbf{u}(\mathbf{x}, t)$ is the velocity vector field at position $\mathbf{x}$ and at time t; $\mathbf{u}(\mathbf{x}, t)$ is integrated across the cross section C_s for which $\mathbf{C_s}$ is the surface vector corresponding to the respective cross section.

To diagnose the haline flux at cross section C_s we define:

$$F_s(t) = \int_{C_s} s(\mathbf{x}, t) \mathbf{u}(\mathbf{x}, t) \cdot \mathbf{dC_s}, \tag{2}$$

where $F_s(t)$ is the haline flux at cross section C_s and $s(\mathbf{x}, t)$ is the salinity field at position $\mathbf{x}$ and at time t.

Matthäus [2006] defines a major saltwater inflow as a flux of salinity higher or equal to 17 PSU across the meridional cross section located at the Darss sill (Figure 1) during five consecutive days in addition to a high stratification condition [*Matthäus*, 2006].

In the present work, the purpose is not to study the occurrence of major saltwater inflows, but rather to quantify changes in the process or occurrence of salt inflows from a general perspective, meaning that not only major salt inflows are taken into account. We therefore modify the criteria of *Matthäus* [2006]. In order to describe the entire flow, we have slightly shifted our Baltic Sea cross section from the Darss Sill toward the east. While we use a similar definition for the inflow salinity, we do not require that a salt inflow should last five consecutive days. However, it is still possible to extract the inflows based on these precise criteria from the diagnostics we define (section 3.3).

We define $s_{inflow}(\mathbf{x}, t)$ as an inflow salinity field which value is:

$$s_{in\,flow}(\mathbf{x}, t) = s(\mathbf{x}, t) \text{ if } s(\mathbf{x}, t) \geq 17PSU$$
$$s_{in\,flow}(\mathbf{x}, t) = 0 \text{ if } s(\mathbf{x}, t) < 17PSU. \tag{3}$$

This definition of $s_{inflow}(\mathbf{x}, t)$ as a field yields the following definitions for the inflowing salt and volume fluxes, respectively:

$$F_{s_{in\,flow}}(t) = \int_{C_s} s_{in\,flow}(\mathbf{x}, t) \mathbf{u}(\mathbf{x}, t) \cdot \mathbf{dC_s}$$
$$F_{v_{in\,flow}}(t) = \int_{C_s} \delta(\mathbf{x}, t) \mathbf{u}(\mathbf{x}, t) \cdot \mathbf{dC_s}, \tag{4}$$

with $\delta(\mathbf{x}, t)$ defined as:

$$\delta(\mathbf{x}, t) = 1 \text{ if } s_{in\,flow}(\mathbf{x}, t) \geq 17PSU$$
$$\delta(\mathbf{x}, t) = 0 \text{ if } s_{in\,flow}(\mathbf{x}, t) < 17PSU. \tag{5}$$
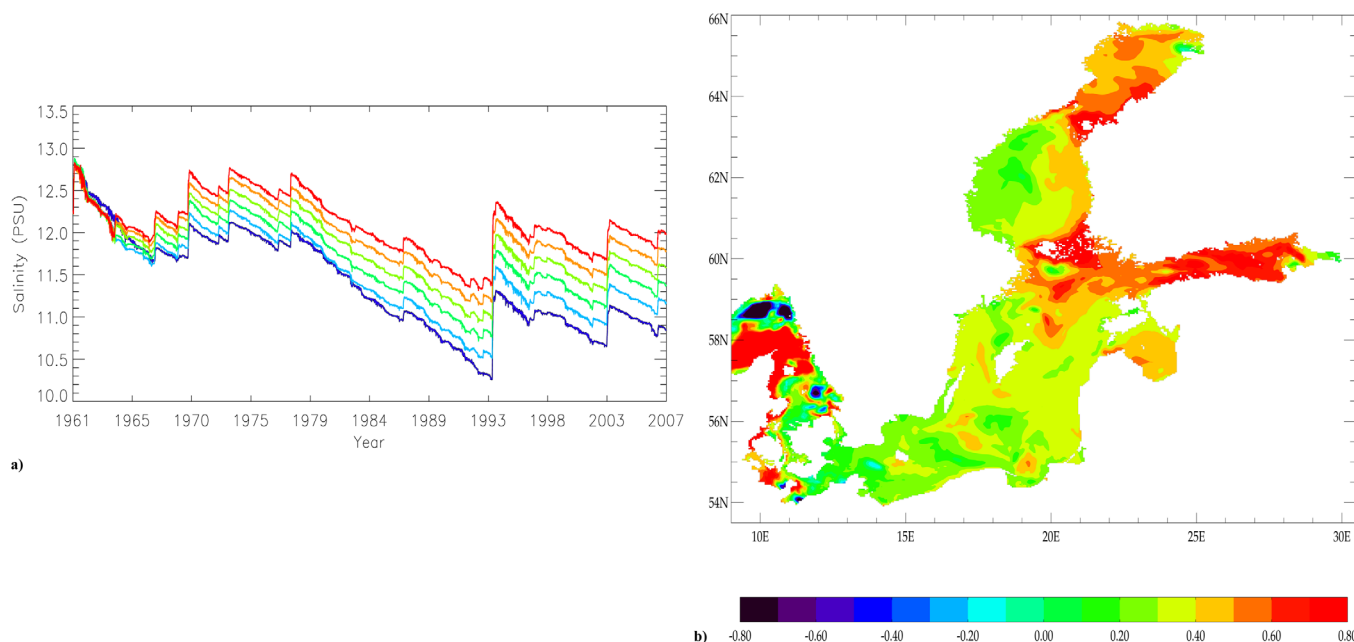
Figure 4. (a) Deep salinity (in PSU) at 250 m at BY15 from 1961 to 2007 for experiments e0, e0.5, e0.75, e1, e1.25, and e1.5, from blue to red, respectively. (b) Comparison of SSS between e1.5 and e0 after 10 years of simulation.

3. Results

Figure 4 depicts the differences in Baltic Sea SSS between the simulations e0 and e1.5 after 10 years of simulation. The Gulf of Finland as well as the Botnian Sea and Bothnian Bay show the most pronounced increases in SSS (Figure 1). The areas of the Baltic Sea with the highest surface salinity increases are disconnected from the North Sea by an area where the surface salinity increase is less pronounced.

Such a spatial pattern can only occur if an increased salt supply has been provided to the lower layers of the Baltic Sea and if some of that salt has found its way back to the surface in places of low stratification through the estuarine baroclinic circulation. The transfer of salinity through the permanent Baltic Sea halocline is a longer process.

Based on this set of sensitivity experiments and on the diagnostics designed in section 2.3, we investigate the reasons behind the increase of salinity of deep water created by a higher mean sea level. Specifically, we set out toward a mechanistic understanding of (1) if a higher mean sea level creates more deep water inflows into the Baltic Sea, or (2) if it increases the magnitude of inflows, or their salinity. Further, we aim to elucidate underlying mechanisms.

3.1. Changes in Intensity of Inflow Events

As a first step, we analyze the changes in the mean intensity of salt inflows and try to understand how underlying processes change from experiments e0 to e1.5. For this purpose we analyze the changes in the mean values of $F_{s_{inflow}}(t)$ and $F_{v_{inflow}}(t)$ from experiments e0 to e1.5, whenever their value is not zero. We thus consider the changes in the inflow characteristics during inflow events.

Applying the diagnostics defined in section 2.3 for the time period 1966–2006 at section S1 yields Figure 5. Figure 5 indicates a clear increase in both strength and frequency of saltwater inflows in e1.5 compared with e0.

The increase of the mean intensity of inflows reaches 5, 7, 14, 17, and almost 24% for experiments e0.5, e0.75, e1, e1.25, and e1.5, respectively, compared with experiment e0.

The percentage of increase of variability of the barotropic flow across section S1 differs from the percentage of increase of intensity of inflows from experiment e0 to experiment e1.5. The percentage of increase of intensity of inflows follows a stronger trend: even if one considers the depth of the critical cross section of
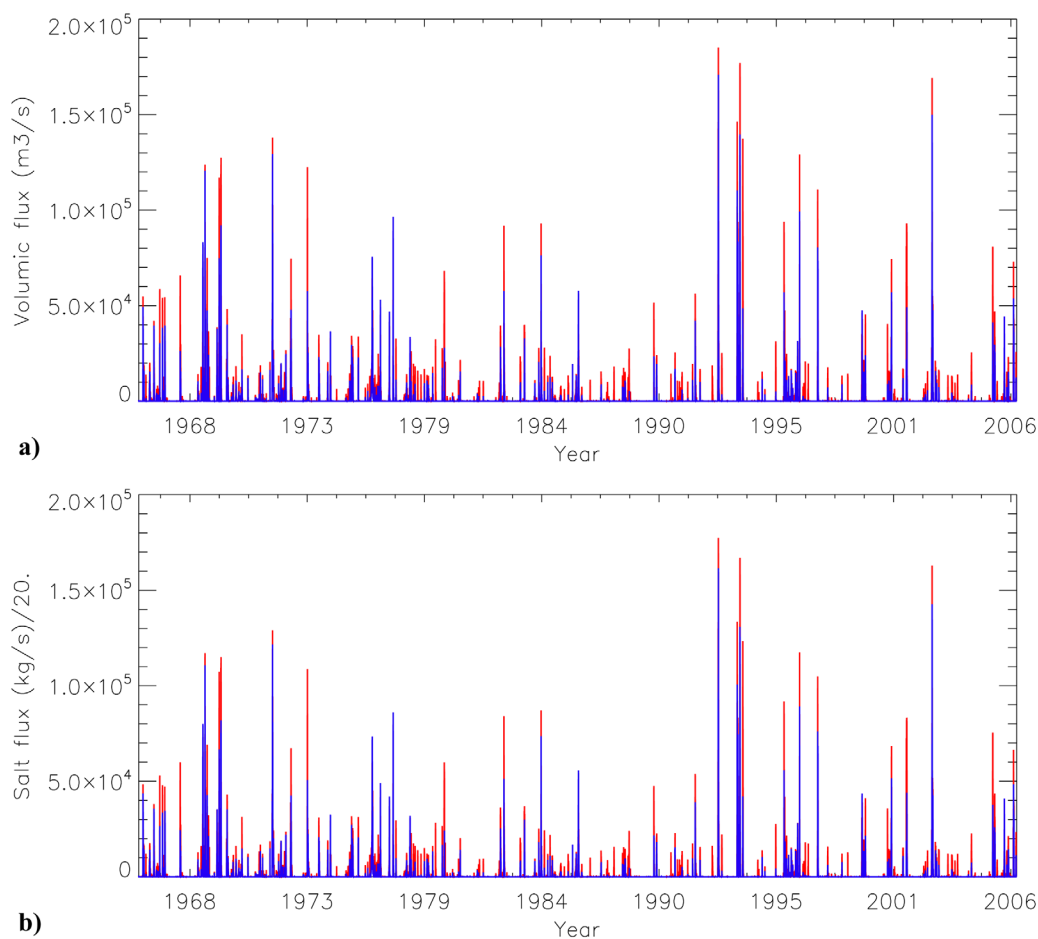
Figure 5. Comparison of volume and salt flux at cross section S1 for the reference experiment e0 (blue) and for the highest sea level increase experiment e1.5 (red). (a) $F_{V_{inflow}}(t)$ in m^3 s^{-1}. (b) $F_{S_{inflow}}(t)$ in kg s^{-1}.

the Great Belt, a sea level rise of 1.5 m creates an increase of the cross section area of only 7%. This fits with the increase of variability of the barotropic flow at section S1, which reaches 6.5% in the model. However, since the increase of intensity of inflows that corresponds to such a sea level rise reaches almost 24%, therefore an additional process must be involved (besides the increase in the cross section) in order to explain the increase of intensity of salt inflows.

A computation of the mean inflowing salinity for all the inflow events of the period and this for each scenario e0, e0.5, e0.75, e1, e1.25, and e1.5 gives, respectively, 18.22, 18.18, 18.18, 18.17, 18.17, and 18.16 PSU. Therefore, the mean salinity of inflow events does not change between the sensitivity runs: the increase in strength and frequency of $F_{S_{inflow}}(t)$ one can notice in Figure 5 is only related with an increase in the strength of the inflows from a volume flux perspective.

3.2. Impact of Sea Level Increase on Mixing in the Danish Straits

Mixing in the Danish Straits is a critical process modulating salt inflows entering the Baltic. Most of the flow that creates salt inflows arrives in the Baltic Sea through the central channel of the Danish Straits (Great Belt) where entrainment rate estimates reach more than 70% [*Kouts and Omstedt*, 1993]. As a consequence, most of the saltier water arriving through the Great Belt is mixed with fresher water, and in a majority of cases is simply mixed with the upper and lighter mass of water, to finally be advected out of the Baltic Sea. Any change of mixing in this area can therefore lead to a dramatic change in the dynamics of saltwater inflows in the Baltic Sea.

Figure 6 shows the percentage of difference in vertical eddy diffusivity between experiments e1.5 and e0 for the Danish Straits area. Vertical eddy diffusivity is represented here as daily mean vertical
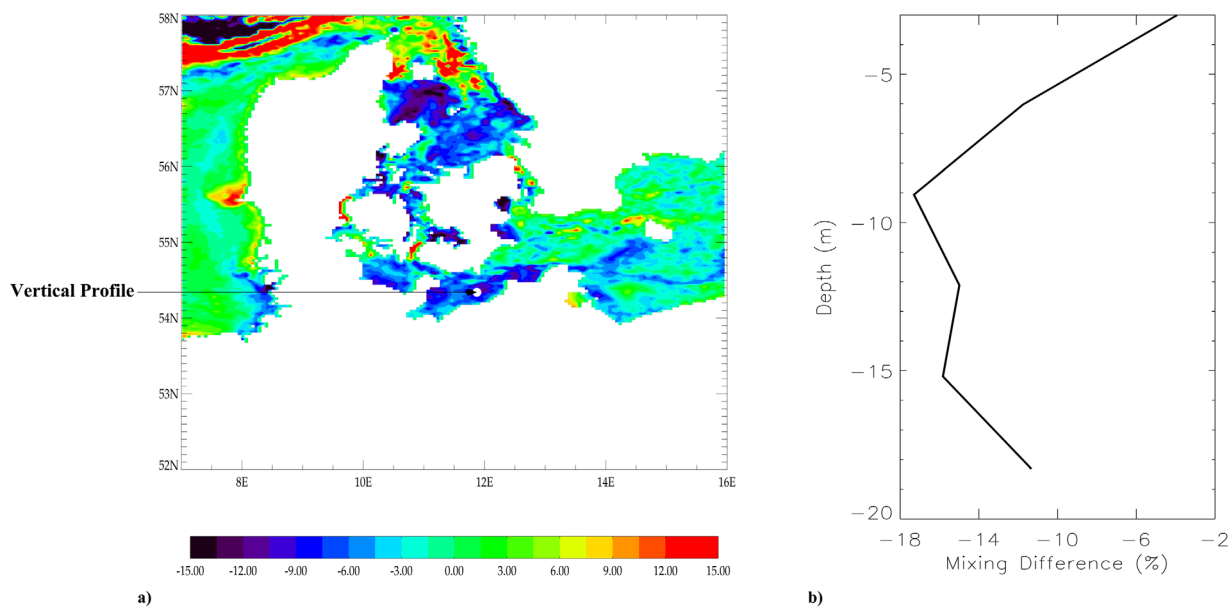
Figure 6. (a) Difference of mean vertically integrated vertical eddy diffusivity for year 1962, in % between experiments e1.5 and e0. (b) Difference of vertical eddy diffusivity at the point shown in the left figure.

turbulent eddy diffusivity as calculated from the $k-\epsilon$ turbulence scheme, and averaged over the whole water column. We show the annual mean difference for 1962. We focus on a year at the beginning of the simulation, because we want to compare the simulations at a similar state of the ocean. In 1962, the state of the ocean is still similar in all sensitivity runs as they are not yet impacted by the differing inflow dynamics.

Figure 6 shows a strong decrease in vertical eddy diffusivity over the entire area of the Danish Straits. The decrease is especially pronounced along the main pathway of salt inflows, the Great Belt and the Darss Sill. Although some slight increase in vertical eddy diffusivity occurs in narrow straits, the mean decrease of vertical eddy diffusivity ranges from 5 to 10% depending on which extent of the Danish Straits area is considered. A decrease of the vertical eddy diffusivity can also be noticed in the South of Kattegat. A pronounced decrease in vertical eddy diffusivity occurs mainly in shallow areas. In deeper regions, a significant increase of vertical eddy diffusivity can be observed.

A vertical profile was chosen in the vicinity of the Darss Sill (Figure 6). There, the utmost damping of vertical eddy diffusivity as a consequence of the rising sea level is approximately 10–15 m below the surface. It is at this depth that the interface between higher fresher water masses and lower saltier water masses is located, and where the entrainment process takes place in the Danish Straits. Entrainment is a critical process of preconditioning the salt inflows in the Baltic Sea. It is still not comprehensively understood, but several studies have been made for the specific case of the Baltic Sea and the region of the Danish Straits. *Kouts and Omstedt* [1993], *Lass and Mohrholz* [2003], and especially *Arneborg et al.* [2007] provide us with the theoretical background which we use in the following.

Based on two different methods, *Arneborg et al.* [2007] computed an estimate of the entrainment parameter E describing the entrainment process that occurs in the Bornholm basin. It can be applied in regions where the flow is strongly influenced by geostrophy, which is the case for the Great Belt region and at the vicinity of section S1.

In their demonstration, *Arneborg et al.* [2007] have defined E as:

$$E = \frac{W_E}{U_s},\qquad(6)$$

where W_E is the entrainment velocity between the lower heavier mass of water, and the upper one of fresher and lighter water. U_s is a velocity explained hereafter.
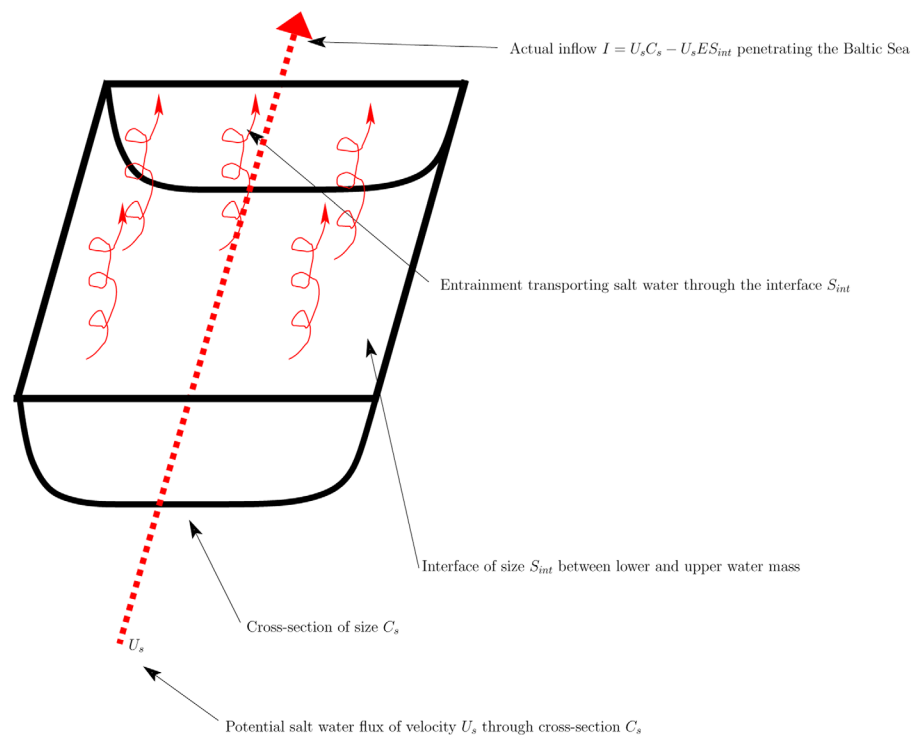
Figure 7. Schematic view of flow I through a cross section C_s of the Danish Straits. A potential inflow of velocity U_s flows below the horizontal section S_{int} located at the interface between ingoing and outgoing flows. This potential inflow is eroded with the entrainment rate E (red curved arrows). U_sC_s (in m³ s⁻¹) is the total volume flux of the potential inflow, I (in m³ s⁻¹) is the actual salt inflow that penetrates the Baltic Sea after the entrainment process that takes place in the Danish Straits has occurred. This entrainment process is described by the entrainment rate E (dimensionless). E describes the effect of deep saline water mixed to the surface where ultimately it will leave the Baltic Sea.

We now assume a system of inflowing water through the Danish Straits to reach a vertical cross section C_s located after the Danish Straits (in the Bornholm basin for example, similar to S1, Figure 1). For this system, we can define (equation (7)):

$$I = U_sC_s - U_sES_{int}, \tag{7}$$

in which I is a volume flux of inflowing water through the cross section C_s with a velocity U_s. S_{int} represents the horizontal surface located at the interface between the mass of inflowing water that can potentially penetrate the Baltic Sea and the lighter water mass located above it. It has an entrainment parameter E (Figure 7). Our model results suggest that the salinity of water masses penetrating the Baltic Sea does not change with sea level rise, but that their frequency or their amplitude does (section 3.1). Hence, we take the point of view that entrainment is a process that erodes potential salt inflows upward, rather than mixing lighter water downward into a potential salt inflow. From a conservation perspective, both points of view are equivalent in our case: A salt inflow being mixed downward with lighter water cannot penetrate the Baltic Sea and will end up in the upper layer on its outgoing journey from the Baltic Sea. In the same manner, a potential salt inflow that is eroded upward mixes with lighter water in the upper layer, does not penetrate the Baltic Sea, and leaves the Baltic Sea.

For any potential salt inflow penetrating through the Danish Straits into the Baltic Sea with a velocity U_s through a strait of cross section C_s, I is the flux that makes it through into the Baltic Sea after the entrainment process has eroded the incoming saltwater flow. This erosion takes place through the halocline of horizontal surface S_{int} with an entrainment rate E. I cannot be negative by definition: if the entrainment is too high, meaning in this case that $ES_{int} > C_s$ then there is no possible inflow. In this case, all the potential inflow of dense water into the Baltic Sea is eroded and I is simply zero. However, for potential inflows making their way into the Baltic Sea, we also know based on literature surveys that most of their content is eroded [*Kouts and Omstedt*, 1993]. Therefore, for our reference experiment e0, this means that we can write:

$$E_0S_{int} = \beta_0C_s, \tag{8}$$

where β_0 is the reference erosion rate for experiment e0, and E_0 the associated entrainment rate. Introducing β_0 allows re-writing the reference volume flux $I(0)$:

$$I(0) = U_s \frac{1-\beta_0}{\beta_0} E_0 S_{int}. \tag{9}$$

We can define E_0, $E_{0.5}$, $E_{0.75}$, E_1, $E_{1.25}$, and $E_{1.5}$ as the entrainment parameters of experiments e0, e0.5, e0.75, e1, e1.25, and e1.5, respectively. We can also define the relative increase of inflowing fluxes $I(h)/I(0)$ during inflow events as:

$$\frac{\delta I(h)}{I(0)} = \frac{S_{int}(E_h - E_0)}{C_s - E_0 S_{int}}, \tag{10}$$

which can be re-written as:

$$\frac{\delta I(h)}{I(0)} = \frac{\beta_0}{1-\beta_0}\left(1 - \frac{E_h}{E_0}\right). \tag{11}$$

Based on the relation found by *Arneborg et al.* [2007], E can be parameterized as (equation (12)):

$$E = a C_d K^b F_r^c, \tag{12}$$

in which $a = 0.084$, $b = 0.6$, $c = 2.65$, C_d is a drag coefficient, K is an estimate of the Ekman number of the flow, and F_r is the baroclinic Froude number. This baroclinic Froude number is defined as:

$$F_r = \frac{U_s}{\sqrt{g'D\cos\alpha_s}}, \tag{13}$$

where g' is the reduced gravity, D the thickness of the lower layer, and α_s is the angle of the slope. The Ekman number of the flow K is defined as (equation (14)):

$$K = \frac{C_d U_s}{f'D}, \tag{14}$$

where C_d is a bottom drag coefficient and $f' = f\cos\alpha$, with f being the Coriolis parameter.

The theory presented by *Arneborg et al.* [2007] is based on a two-layer system. At the entrance of the Baltic Sea, we can assume that sea level rise affects only the lower layer of the system since the thickness of the upper one comes from the amount of river runoff rejected into the Baltic Sea and its eventual mixing within the basin. The thickness of the lower D is what varies in case of a mean variation of sea level. Based on the formulation of the entrainment parameter E and its relation with the Froude and Ekman numbers, equation (11) can be rewritten as:

$$\frac{\delta I(h)}{I(0)} = \frac{\beta_0}{1-\beta_0}\left(1 - \left(\frac{D_0}{D_h}\right)^{1.925}\right), \tag{15}$$

where D_0 is the thickness of the lower layer for the reference experiment e0, and D_h is the thickness of the lower layer for an experiment of mean sea level rise h. Based on a thickness D_0 of 12 m as in *Arneborg et al.* [2007], we compute the increase of inflow intensity predicted by this simple method and compare it to that predicted by our set of experiments for mean sea level increases of 0.5–1.5 m.

Since rising sea level additionally impacts the inflows by enlarging the cross section S1, we additionally depict these anticipated changes in Figure 8. In order to get realistic results from this simple box model, we set $\beta_0 = 0.5$ which is lower than even the lower bound (0.7) suggested by *Kouts and Omstedt* [1993]. However, the results of *Kouts and Omstedt* [1993] use a conceptual model based on long-term measurements, while we apply a 3-D ocean model that has a tendency to overestimate the stratification at the base of the mixed layer.

We notice that the increase of intensity of salt inflows follows the theory of *Arneborg et al.* [2007] for low sea level rise values. However, for higher sea level rise the addition of the barotropic variability at section S1 to the flow predicted by this theory provides a range that fits better with what is predicted by the model. When we extend our definition of inflows following the criterion of *Matthäus* [2006] which accounts for inflows only if they last at least five consecutive days then the results are different: the increasing trend follows closely that of the increase in barotropic variability at section S1.
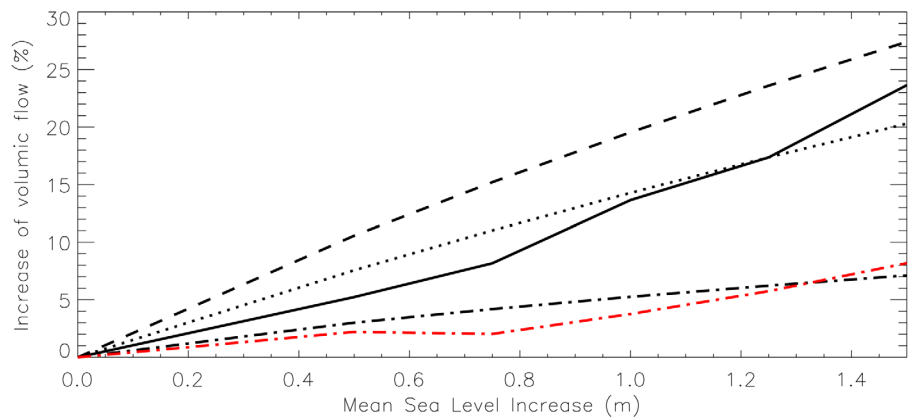
Figure 8. Plain line = mean volume inflow increase (%) for mean sea level increases of 0.5–1.5 m in simulations from e0 to e1.5. Dash-dotted line = increase in barotropic flow standard deviation (%) for the same set of experiments. Dotted line = $\delta I(h)/I(0)$ as computed in equation (15). Dashed line = $\delta I(h)/I(0)$ as computed in equation (15) to which the increase in barotropic flow standard deviation is added. Red dash-dotted line = increase in major Baltic Sea inflows (consecutive five day criteria taken into account).

3.3. Analysis of the Frequency of Inflow Events

So far we have concentrated on how the volume flux per inflow day changes with sea level rise. We now also present results on the number of inflow events and the increase in duration of the inflows. Our results indicate an increase in the number of days during which an inflow occurs, and additionally an increase in the mean duration of inflow events. This change is more difficult to address since it contains a higher degree of nonlinearity. It represents a change between a process (an inflow) that can exist and that is driven by an increase of sea level, and no inflow if no sea level increase occurs.

We present both the percentage of changes for the case of all salt inflow events (Figure 9), and the case of major Baltic Sea inflows with a duration of at least 5 days (Figure 10). In both cases, the number of salt inflows and the duration of salt inflows increase. The number of relatively short inflows (less than 5 days), which was already quite high, increases by a maximum of only 10%. In the same manner, major Baltic Sea inflows increase in length only by a maximum factor of 15% for a sea level rise of 1.5 m.

4. Discussion and Conclusion

In the present study, we investigate the effect of expected changes in global mean sea level on the processes governing salt inflows into the Baltic Sea. We show that a moderate mean sea level rise modifies the long-term dynamics of salt inflows in the Baltic Sea.
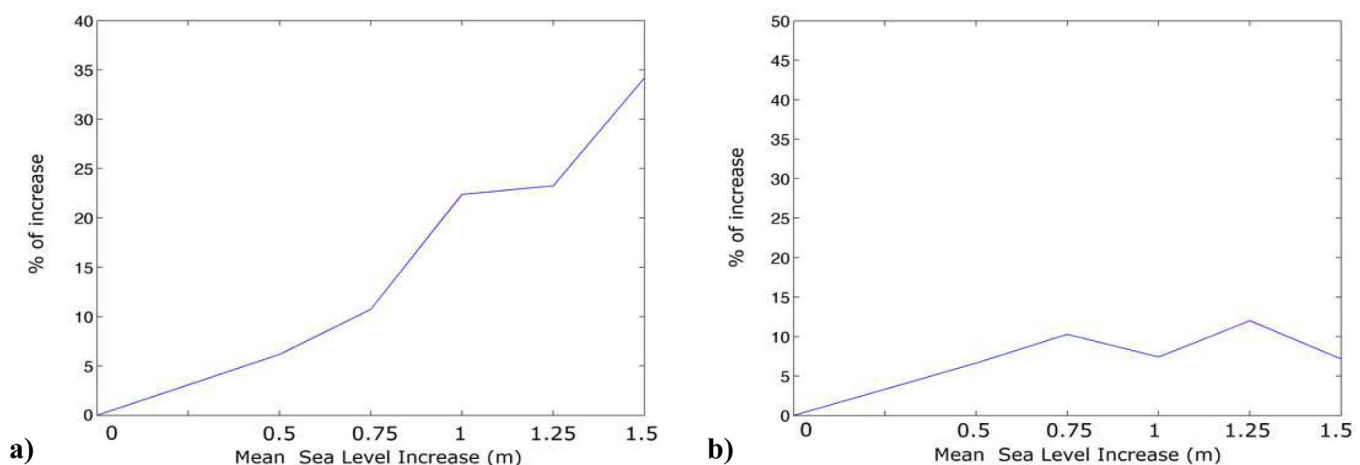

Figure 9. (a) Percentage of increase of length for salt inflow events of at least 1 day. (b) Percentage of increase in number of salt inflow events of at least 1 day.
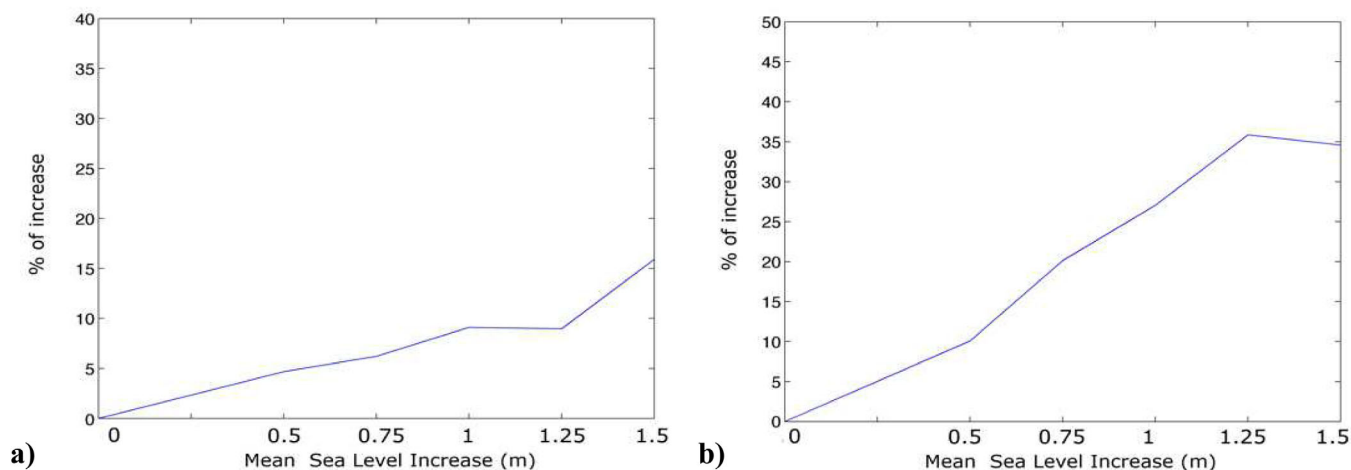
Figure 10. (a) Percentage of increase of length for salt inflow events of at least 5 days. (b) Percentage of increase in number of salt inflow events of at least 5 days.

In a 46 year hindcast simulation of NEMO-Nordic, the bottom salinity in the deepest parts of the Baltic Sea increases by 0.3 PSU for an anticipated sea level rise of 0.5 m. This salinity increase reaches values of more than 1 PSU for a mean sea level rise of 1.5 m. These increases in the deep salinity indicate an increase in the ventilation of the deep parts of the Baltic Sea even for a modest sea level rise.

Sea level rises trigger deep salinity biases, but no diverging temporal trends. Hence, apparently, on the time scales and magnitudes considered here, increased deep salinity does not weaken consecutive inflows.

We conclude that our results are robust, even though NEMO-Nordic overestimates the ventilation of intermediate layers and underestimates salinity transport to the deepest layers. Based on the argument that these model biases would rather weaken the simulated changes in the inflows instead of overestimating them, the model has a tendency to under estimate the amount of inflowing water that reaches the deepest parts of the Baltic Sea. It is the result of the vertical coordinate system and occurs mostly at shelf breaks: despite the bottom boundary layer parameterization, the model has difficulties representing slope currents in shelf break regions. This suggests that the model should also underestimate the impact of larger water masses penetrating the Baltic Sea.

Even though we illustrate the saltwater inflows become more frequent, longer, and more intense, we focus with our in-depth analysis on the intensity of inflows. Comparing compare the theoretical approach suggested by *Arneborg et al.* [2007] with the results of NEMO-Nordic, we find that:

1. The theoretical model presented by *Arneborg et al.* [2007] fits generally well for a given reference rate of erosion which is below that of observed values and with the simulated inflow increase for sea level rise from 0.5 to 1 m This indicates that the inflow intensities were mainly impacted by a decrease of entrainment for these values. The increase of cross-sectional area does not appear to play a significant role for this range of sea level increase: the increase in the volume per day of saltwater inflows is much larger than the increase in standard deviation of the barotropic flow at section S1.

2. For larger anticipated mean sea level rise ranges, from 1.25 to 1.5 m, and beyond if one considers the slopes of curves of Figure 8, the reduction of entrainment in the Danish Straits alone cannot explain the increase in Baltic Sea salt inflows. This suggests the importance of another process. Adding the increase in standard deviation of the barotropic flow to the increase of inflows estimated from the reduction of the entrainment provides estimates of the increase in inflows that fit better to model results. This suggests that these two processes may simply add up (Figure 8) in the case of sea level rises exceeding 1.25 m. It is beyond the scope of this article to disentangle the respective contributions of the reduced entrainment and of the increased cross sections in the Danish Straits; also, because a comprehensive answer calls for an improved, higher-resolved representation of the Danish Straits. Further studies involving a better horizontal resolution of the Danish Straits area is therefore required.

3. If we consider only major inflows, as defined by *Matthäus* [2006], the highest-case scenario increases such inflows by 8%. In that case the increase of inflowing volume is highly correlated with the increase in standard deviation (Figure 8, red curve). As explained by *Schimanke et al.* [2014], major Baltic Sea inflows

are, to first order, barotropic phenomena driven by an emptying-refilling process of the Baltic Sea. As such they feature a lower sensitivity to a decrease of the mixing in the Danish Straits, and a rather high correlation with the increase in barotropic variability (which, in turn, is caused by the increase in cross section in the Danish Straits).

4. The decrease of mixing in the Danish Straits gives this area a stronger baroclinic behavior. This decrease of mixing enables stronger small inflows. The increase in cross section on the other hand affects the barotropic behavior of the Danish Straits, by also enabling stronger small inflows but also stronger major salt inflows into the Baltic Sea.

If we consider the changes of frequency and duration of inflow events, our results show an increase in the number of days during which inflow events occur, and indicate that the mean length of inflow events is affected regardless of the criteria that is chosen. The increase of frequency of major salt inflows reaches up to 35% for a mean sea level rise of 1.5 m, but their length increases only by a maximum of 15%.

For the rather frequent short inflow events, the frequency of inflows increases only by less than 10% for the most extreme case of sea level rise, but their length, that has more potential to become longer, increases by about 35%. It is difficult to interpret these findings which represent rather time-integrated metrics (in contrast to the previously presented dealt with volume fluxes). Even though, we conclude that the decrease of mixing is an essential factor determining the increase of frequency and length of Baltic Sea salt inflows: First, a decrease of mixing raises the probability that an inflowing water mass can penetrate through the Danish Straits and preserve its properties, hence increasing the probability of creating a salt inflow. Second, reduced mixing implies that the water masses at the beginning and at the end of the inflow process also have a larger probability to cross the Danish Straits while preserving their properties, thus increasing the duration of an inflow event.

This latter aspect and the effect of sea level rise on the overall haline structure of the Baltic Sea (i.e., which layers become saltier due to which process related with sea level rise), is an aspect we will further investigate in addition to the coupling of stronger salt inflows with biogeochemistry. From this perspective, it is difficult to make a forecast just based on these results. However, one can expect the following features. First, added saltwater inflows usually carry oxygen to the deepest parts of the Baltic Sea, but this added oxygen content is usually consumed within a time scale of 1 or 2 years [*Nausch et al.*, 2008]. However, added salinity in the deepest parts of the Baltic Sea also leads to stronger stratification which suggests on longer time periods that the oxygen content might actually decrease. A consequence could be a higher release of phosphorus from the bottom sediments [*Almroth-Rosell et al.*, 2015]. From this point of view, further investigation with the use of a coupled biogeochemistry model is our next target.

References

Adcroft, A., and J.-M. Campin (2004), Re-scaled height coordinates for accurate representation of free-surface flows in ocean circulation model, *Ocean Modell.*, *7*, 269–284.

Almroth-Rosell, E., K. Eilola, I. Kuznetsov, P. O. Hall, and H. M. Meier (2015), A new approach to model oxygen dependent benthic phosphate fluxes in the Baltic Sea, *J. Mar. Syst.*, *144*, 127–141.

Arneborg, L., V. Fiekas, L. Umlauf, and H. Burchard (2007), Gravity current dynamics and entrainment—A process study based on observations in the Arkona Basin, *J. Phys. Oceanogr.*, *37*, 2094–2113, doi:10.1175/JPO3110.1.

Axell, L., R. Hordoir, A. Jönsson, S. de Koster, Y. Liu, P. Ljungemyr, and P. Strömberg (2014), Verification of NEMO-Nordic: A setup for the Baltic Sea, technical report, Swed. Meteorol. and Hydrol. Inst.

Beckmann, A., and R. Döscher (1997), A method for improved representation of dense water spreading over topography in geopotential-coordinate models, *J. Phys. Oceanogr.*, *27*, 581–591.

Blank, R., J. Lubchenco, and R. Dietrick (2012), Global sea level rise scenarios for the united states national climate assessment, *NOAA Tech. Rep. OAR CPO-1*, Natl. Oceanic and Atmos. Admin., Clim. Program Off., Silver Spring, Md.

Dietze, H., U. Löptien, and K. Getzlaff (2014), MOMBA 1.1—A high-resolution Baltic Sea configuration of GFDL's modular ocean model geoscientific model development, *Geosci. Model Dev.*, *7*, 1713–1731, doi:10.5194/gmd-7-1713-2014.

Egbert, G., A. Bennett, and M. Foreman (1994), TOPEX/POSEIDON tides estimated using a global inverse model, *J. Geophys. Res.*, *99*(C12), 24,821–24,852, doi:10.1029/94JC01894.

Egbert, G. D., and S. Y. Erofeeva (2002), Efficient inverse modeling of barotropic ocean tides, *J. Atmos. Oceanic Technol.*, *19*(2), 183–204, doi:10.1175/1520-0426.

Eilola, K., and A. Stigebrandt (1998), Spreading of juvenile freshwater in the Baltic proper, *J. Geophys. Res.*, *103*(C12), 27,795–27,807.

Ekman, M., and J. Mäkinen (1996), Mean sea surface topography in the Baltic Sea and its transition area to the North Sea: A geodetic solution and comparisons with oceanographic models, *J. Geophys. Res.*, *101*(C5), 11,993–11,999, doi:10.1029/96JC00318.

Funkquist, L., and E. Kleine (2007), HIROMB: An introduction to HIROMB, an operational baroclinic model for the Baltic Sea, *Rep. Oceanogr.*, *37*, Swed. Meteorol. and Hydrol. Inst., Norrköping, Sweden.

Galperin, B., L. H. Kantha, S. Hassid, and A. Rosati (1988), A quasi-equilibrium turbulent energy model for geophysical flows, *J. Atmos. Sci.*, *45*, 55–62.

Godhe, A., J. Egardt, D. Kleinhans, L. Sundqvist, R. Hordoir, and P. Jonsson (2013), Seascape analysis reveals regional gene flow patterns among populations of a marine planktonic diatom, *Proc. R. Soc. B*, *280*, doi:10.1098/rspb.2013.1599.

Gogina, M., and M. L. Zettler (2010), Diversity and distribution of benthic macrofauna in the Baltic Sea: Data inventory and its use for species distribution modelling and prediction, *J. Sea Res.*, *64*(3), 313–321.

Hordoir, R., and H. E. M. Meier (2010), Freshwater fluxes in the Baltic Sea—A model study, *J. Geophys. Res.*, *115*, C08028, doi:10.1029/2009JC005604.

Hordoir, R., C. Dieterich, C. Basu, H. Dietze, and M. Meier (2013), Freshwater outflow of the Baltic Sea and transport in the Norwegian current: A statistical correlation analysis based on a numerical experiment, *Cont. Shelf Res.*, *64*, 1–9, doi:10.1016/j.csr.2013.05.006.

IPCC (2013), Climate change 2013: The physical science basis, in *Working Group I Contribution to the Fifth Assessment Report*, edited by R. Feistel, G. Nausch, and N. Wasmund, *Rep. WGI AR5*. Tech. Support Unit, Univ. of Bern, Bern.

Kouts, T., and A. Omstedt (1993), Deep water exchange in the Baltic proper, *Tellus, Ser. A*, *45*, 331–324.

Large, W. G., and S. Yeager (2004), Diurnal to decadal global forcing for ocean and sea-ice models: The data sets and flux climatologies, *NCAR Tech. Note*, *NCAR/TN-460+STR*, CGD Div. of the Natl. Cent. for Atmos. Res.

Lass, H. U., and W. Matthäus (1996), On temporal wind variations forcing salt water inflows into the Baltic Sea, *Tellus, Ser. A*, *48*, 663–671, doi:10.1034/j.1600-0870.1996.t01-4-00005.x.

Lass, H. U., and V. Mohrholz (2003), On dynamics and mixing of inflowing saltwater in the Arkona Sea, *J. Geophys. Res.*, *108*(C2), 3042, doi:10.1029/2002JC001465.

Leclair, M., and G. Madec (2009), A conservative leapfrog time stepping method, *Ocean Modell.*, *30*, 88–94, doi:10.1016/j.ocemod.2009.06.006.

Levitus, S., and T. P. Boyer (1994), Salinity, in *World Ocean Atlas 1994, NOAA Atlas NESDIS*, vol. 3, 99 pp., U.S. Gov. Print. Off., Washington, D. C.

Löptien, U., and H. E. M. Meier (2011), The influence of increasing water turbidity on the sea surface temperature in the Baltic Sea: A model sensitivity study, *J. Mar. Syst.*, *88*(2), 323–331, doi:10.1016/j.jmarsys.2011.06.001.

Löptien, U., S. Martensson, H. E. M. Meier, and A. Höglund (2013), Long-term characteristics of simulated ice deformation in the Baltic Sea (1962-2007), *J. Geophys. Res. Oceans*, *118*, 801–815, doi:10.1002/jgrc.20089.

Madec, G. (2010), NEMO ocean engine, version 3.3, *Note du Pôle de modélisation de l'Inst. Pierre-Simon Laplace 27*, Inst. Pierre-Simon Laplace, Paris. [Available at http://www.nemo-ocean.eu/.]

Matthäus, W. (2006), The history of investigation of salt water inflows in the Baltic Sea—From the early beginning to recent results, *Mar. Sci. Rep. 65*, Baltic Sea Res. Inst. (IOW), Ger. Inst. für Ostseeforschung Warnemünde, Rostock.

Meier, H., R. Hordoir, H. Andersson, C. Dieterich, K. Eilola, B. Gustafsson, A. Höglund, and S. Schimanke (2012), Modeling the combined impact of changing climate and changing nutrient loads on the Baltic Sea environment in an ensemble of transient simulations for 1961-2099, *Clim. Dyn.*, *39*(9–10), 2421–2441, doi:10.1007/s00382-012-1339-7.

Meier, H. E. M. (2007), Modeling the pathways and ages of inflowing salt- and freshwater in the Baltic Sea, *Estuarine Coastal Shelf Sci.*, *74*, 717–734.

Meier, H. E. M., and F. Kauker (2003), Modeling decadal variability of the Baltic Sea: 2. Role of freshwater inflow and large-scale atmospheric circulation for salinity, *J. Geophys. Res.*, *108*(C11), 3368, doi:10.1029/2003JC001799.

Meier, H. E. M., R. Döscher, and T. Faxén (2003), A multiprocessor coupled ice-ocean model for the Baltic Sea: Application to salt inflow, *J. Geophys. Res.*, *108*(C8), 3273, doi:10.1029/2000JC000521.

Meier, H. E. M., E. Kjellström, and L. P. Graham (2006), Estimating uncertainties of projected Baltic Sea salinity in the late 21st century, *Geophys. Res. Lett.*, *33*, L15705, doi:10.1029/2006GL026488.

Nausch, G., R. Feistel, and N. Wasmund (2008), *State and Evolution of the Baltic Sea, 1952-2005: A Detailed 50-Year Survey of Meteorology and Climate, Physics, Chemistry, Biology, and Marine Environment*, John Wiley, Hoboken, N. J.

Pfeffer, W. T., J. T. Harper, and S. O'Neel (2008), Kinematic constraints on glacier contributions to 21st-century sea-level rise, *Science*, *321*, 1340–1343, doi:10.1126/science.1159099.

Samuelsson, P., C. Jones, U. Willén, U. Ullerstig, S. Golvik, U. Hansson, C. Jansson, E. Kjellström, G. Nikulin, and K. Wyser (2011), The Rossby centre regional climate model RCA3: Model description and performance, *Tellus, Ser. A*, *63*, 4–23.

Schimanke, S., C. Dieterich, and H. E. M. Meier (2014), An algorithm based on sea-level pressure fluctuations to identify major Baltic inflow events, *Tellus, Ser. A*, *66*, doi:10.3402/tellusa.v66.23452.

Stigebrandt, A., R. Rosenberg, L. Råman Vinnå, and M. Ödalen (2014), Consequences of artificial deepwater ventilation in the Bornholm Basin for oxygen conditions, cod reproduction and benthic biomass—A model study, *Ocean Sci. Discuss.*, *11*(4), 1783–1827, doi:10.5194/osd-11-1783-2014.

Umlauf, L., and H. Burchard (2003), A generic length-scale equation for geophysical turbulence models, *J. Mar. Syst.*, *61*, 235–265.

Vancoppenolle, M., T. Fichefet, H. Goosse, S. Bouillon, G. Madec, and M. A. M. Maqueda (2008), Simulating the mass balance and salinity of arctic and Antarctic sea ice, *Ocean Modell.*, *27*(1–2), 33–53, doi:10.1016/j.ocemod.2008.10.005.